PROCEEDINGS OF SPIE

SPIEDigitalLibrary.org/conference-proceedings-of-spie

Integrated photoacoustic and fluorescence confocal microscopy

Yu Wang, Konstantin Maslov, Chulhong Kim, Song Hu, Lihong V. Wang

Yu Wang, Konstantin Maslov, Chulhong Kim, Song Hu, Lihong V. Wang, "Integrated photoacoustic and fluorescence confocal microscopy," Proc. SPIE 7899, Photons Plus Ultrasound: Imaging and Sensing 2011, 78990M (17 February 2011); doi: 10.1117/12.874888

SPIE.

Event: SPIE BiOS, 2011, San Francisco, California, United States

Integrated photoacoustic and fluorescence confocal microscopy

Yu Wang, Konstantin Maslov, Chulhong Kim, Song Hu, Lihong V. Wang*
Department of Biomedical Engineering, Washington University in St. Louis, Campus Box 1097,
One Brookings Drive, St. Louis, MO 63130

ABSTRACT

Optical-resolution photoacoustic microscopy has demonstrated utility in imaging and characterizing microvasculature networks in vivo. This work presents a novel imaging system that integrates optical-resolution photoacoustic microscopy and fluorescence confocal microscopy for simultaneous photoacoustic and fluorescence imaging. The integrated system can acquire intrinsically registered photoacoustic and fluorescence images in a single scan. Capable of providing micrometer scale microscopic imaging of both optical absorption and fluorescence contrasts, the system demonstrates *in vivo* imaging of oxygen saturation and oxygen partial pressure in mouse ears.

Keywords: Photoacoustic microscopy, fluorescence confocal microscopy, oxygen saturation, oxygen partial pressure

1. INTRODUCTION

Optical resolution photoacoustic microscopy (PAM) is a noninvasive volumetric imaging method predominantly sensitive to optical absorption [1-4]. It is able to acquire micrometer resolution images *in vivo* using endogenous absorption contrast, such as hemoglobin and melanin. Noninvasively imaging of both hemoglobin concentration and oxygen saturation in single blood vessels using PAM has been demonstrated. Other common forms of optical imaging modalities, such as optical coherence tomography (OCT) and fluorescence confocal microscopy (FCM) are based on optical scattering or fluorescence contrasts, respectively. Structural and functional images based on these different imaging contrasts provide complementary information for biological studies.

PAM and OCT have been combined previously for multimodal retina imaging [5]. It provides volumetric imaging of the retinal microvasculature using PAM and the retinal structure using OCT. Here, we developed a dual-modality imaging system which integrates photoacoustic microscopy and fluorescence confocal microscopy (PA-FCM). Co-registered images of optical absorption contrast and fluorescence contrast can be acquired simultaneously. By imaging fluorophore, FCM can provide not only rich context for PAM vasculature imaging, but also complementary functional information for more comprehensive insights into physiology.

To demonstrate the PA-FCM system, we imaged the hemoglobin oxygen saturation (sO_2) using PAM and oxygen partial pressure (pO_2) using FCM *in vivo* in single blood vessels. In addition, PAM also mapped the total hemoglobin concentration (HbT) at the isosbestic wavelength. The multimodal microscopy system shows that the PAM system can be naturally integrated to FCM system which is one of the traditional optical image modalities. The natural combination of PAM and FCM is anticipated to encourages the commercialization of PAM imaging technique as a supplement of the mainstream optical imaging techniques for routine laboratory use.

2. METHOD AND METERIALS

2.1 PA-FCM system configuration

The experimental configuration of our PA-FCM system is shown in figure 1 [6]. The system utilizes a wavelength-tunable dye laser (CBD-D, Sirah) pumped by a Nd:YLF laser (INNOSLAB, Edgewave). Laser pulses from the dye laser (560 nm to 590 nm) are used to image hemoglobin absorption at multiple wavelengths. To excite the oxygen-sensitive phosphores, the 523 nm pump laser pulses are delivered into the microscope system. The laser pulse illuminating the sample has a pulse energy of ~ 100 nJ. Chromophores in the sample generate photoacoustic wave and/or fluorescence light after absorbing the excitation laser pulse. Photoacoustic waves and fluorescence lights are separated by an acoustic-optical beam splitter. A 75 MHz ultrasonic transducer (V2022BC, Olympus NDT) is used to detect the PA waves. The

Photons Plus Ultrasound: Imaging and Sensing 2011, edited by Alexander A. Oraevsky, Lihong V. Wang,
Proc. of SPIE Vol. 7899, 78990M · © 2011 SPIE · CCC code: 1605-7422/11/$18 · doi: 10.1117/12.874888

fluorescence light after passing through the filter is collected by a photomultiplier tube module (H6780-20, Hamamatsu). The FCM subsystem use a 150 µm diameter detection pinhole to suppress the out-of-focus light. The photoacoustic and fluorescence signals are digitized and stored by a DAQ instrument (CS 14200, Gage Applied).

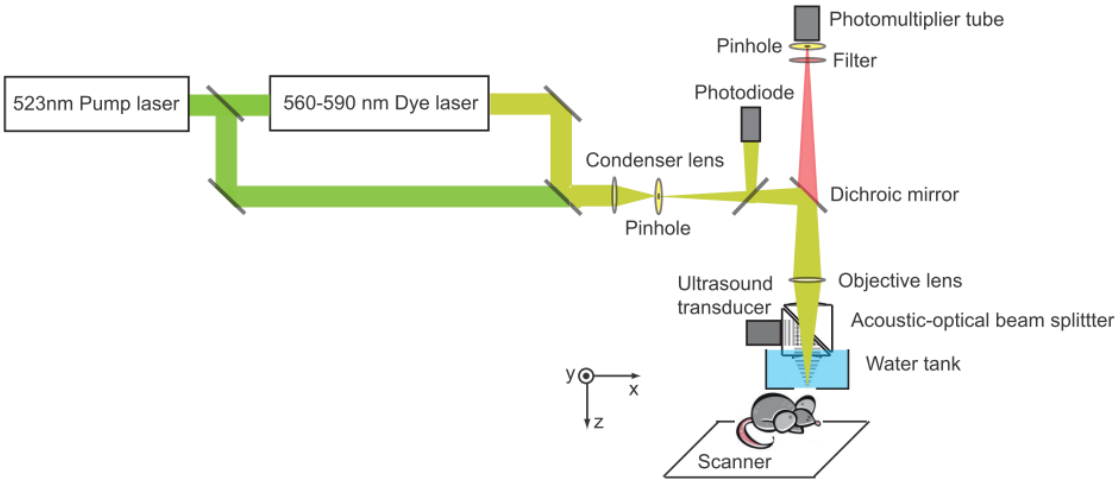

Figure 1. Schematic of the integrated photoacoustic and fluorescence confocal microscopy system.

2.2 PA-FCM system spatial resolution

The spatial resolution of the PAM subsystem was measured experimentally by imaging a surgical blade. The lateral resolution of PAM, determined by the objective lens NA, is estimated to be ~3.9 µm. The axial resolution of PAM is measured to be ~17 µm, as limited by the 100 MHz bandwidth of the ultrasonic transducer. We quantified the spatial resolution of the FCM subsystem by imaging a mirror surface. The experimental data yields a lateral resolution of ~3.9 µm and a axial resolution of ~38 µm (Table 1).

Table 1. Spatial resolution of the integrated PA-FCM system.

Modality	Transverse resolution	Axial resolution	Contrast
Fluorescence confocal microscopy	3.9 µm	17 µm	Fluorescence
Photoacoustic microscopy	3.9 µm	38 µm	Optical absorption

2.3 *In vivo* mapping of sO_2 and pO_2

Understanding of oxygen consumption and delivery *in vivo* requires the development of imaging techniques for mapping the intravascular oxygen concentration. Oxygen in blood is either dissolved or bound to hemoglobin. pO_2 quantifies the concentration of dissolved oxygen which is directly available to cell; sO_2 quantifies the amount of oxygen bound to hemoglobin.

PAM subsystem can measure sO_2 by spectroscopically measuring hemoglobin absorption [1].

$$\mu_a(\lambda_i) = \varepsilon_{Hbr}(\lambda_i)[Hbr] + \varepsilon_{HbO_2}(\lambda_i)[HbO_2] \quad (1)$$

where μ_a is the hemoglobin optical absorption measured by PAM, ε_{HbO_2} and ε_{Hbr} are the molar extinction coefficients of oxygenated and deoxygenated hemoglobin, and λ is the laser wavelength. By a radiometric procedure

$$sO_2 = \frac{[HbO_2]}{[HbO_2]+[Hbr]}, \quad (2)$$

sO_2 value can be calculated pixel by pixel.

FCM subsystem can measure pO_2 using phosphorescence lifetime quenching technique [7-10]. Oxygen-sensitive Pd-porphyrin phosphorescence probe is injected into the systemic vasculature. The phosphorescence is quenched by intravascular oxygen. The relationship of phosphorescence lifetime and the pO_2 follows the Stern-Volmer equation

$$\frac{1}{\tau} = \frac{1}{\tau_0} + k_q[pO_2], \quad (3)$$

where τ_0 is the phosphorescence lifetime without oxygen quenching and k_q is the quenching constant calibrated *in vitro*[11]. In our studies, we used the oxygen-sensitive probe, Pd-meso-tetra (4-carboxyphenyl) porphyrin (PdT790, Frontier Scientific). It has a peak absorption wavelength of 524 nm. The PdT790 (10 mg/ml) was conjugated with bovine serum albumin (60 mg/ml) in 0.9% NaCl solution to prevent its leakage from the vasculature. We injected a 0.1 ml volume of phosphorescent probe solution through the tail vein. Images were acquired 10 min after injection to allow the probe to equilibrate in the blood.

3. RESULTS AND DISCUSSION

We imaged nude mouse ears to demonstrate the dual-modality microscopy of sO_2 and pO_2 in vivo. All experimental animal procedures were carried out in conformity with the laboratory animal protocol approved by the Animal Studies Committee of Washington University in St. Louis.

The photoacoustic image of the mouse ear vasculature were acquired at two wavelengths of 570 nm and 578 nm. At the isosbestic wavelength of 570 nm (Fig. 2(a)), the HbO_2 and Hbr have the same molar extinction coefficients. Hence, the photoacoustic signal amplitudes measure the total hemoglobin concentration (HbT). Photoacoustic image at 578 nm was also acquired. Aided by the molar extinction spectra of HbO_2 and Hbr, intravascular sO_2 level is computed as shown in Fig. 2(b). In the sO_2 mapping, the arterioles and venules are pseudo-colored in red and blue based on their different sO_2 levels [12].

Figure 3 (a) shows the FCM image of the mouse ear after injection of the Pd-porphyrin probe. The sebaceous glands and vasculature can be seen in images as dot and tree features. The autofluorescence from the glands has nanosecond-scale lifetime while the phosphorescence lifetime of the Pd-porphyrin probe is ~100 μs. Thus we can separate the images of sebaceous glands and vasculature by splitting the FCM signal in time domain. Figure 3(b) and 3(c) show the time-integrated FCM images in the range of 0-5 μs and 5-500 μs. The latter one shows the blood vasculature based on the phosphorescence contrast. In the regions indicated by the arrows, the phosphorescence lifetime in artery (105 μs) is shorter than that in the vein (141 μs). Using Stern-Volmer equation, the shorter lifetime can be converted to a higher arterial pO_2 level, which agrees with the known physiology.

Fitting of the phosphorescence decay at each scanning step gives the lifetime mapping as shown in figure 4(a). Subsequently, mapping of intravascular pO_2 (Fig. 4(b)) is generated using Eq. 3. In the pO_2 mapping, the arterioles and venules can be distinguished by different pO_2 levels.

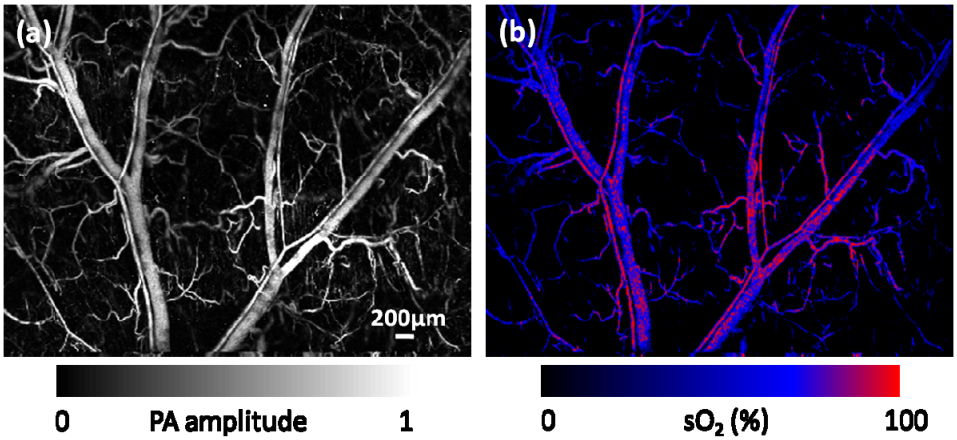

Figure 2. PAM imaging of a mouse ear *in vivo*. (a) Photoacoustic image of total concentration of hemoglobin acquired at the isosbestic wavelength of 570 nm. (b) Photoacoustic image of sO_2 mapping.

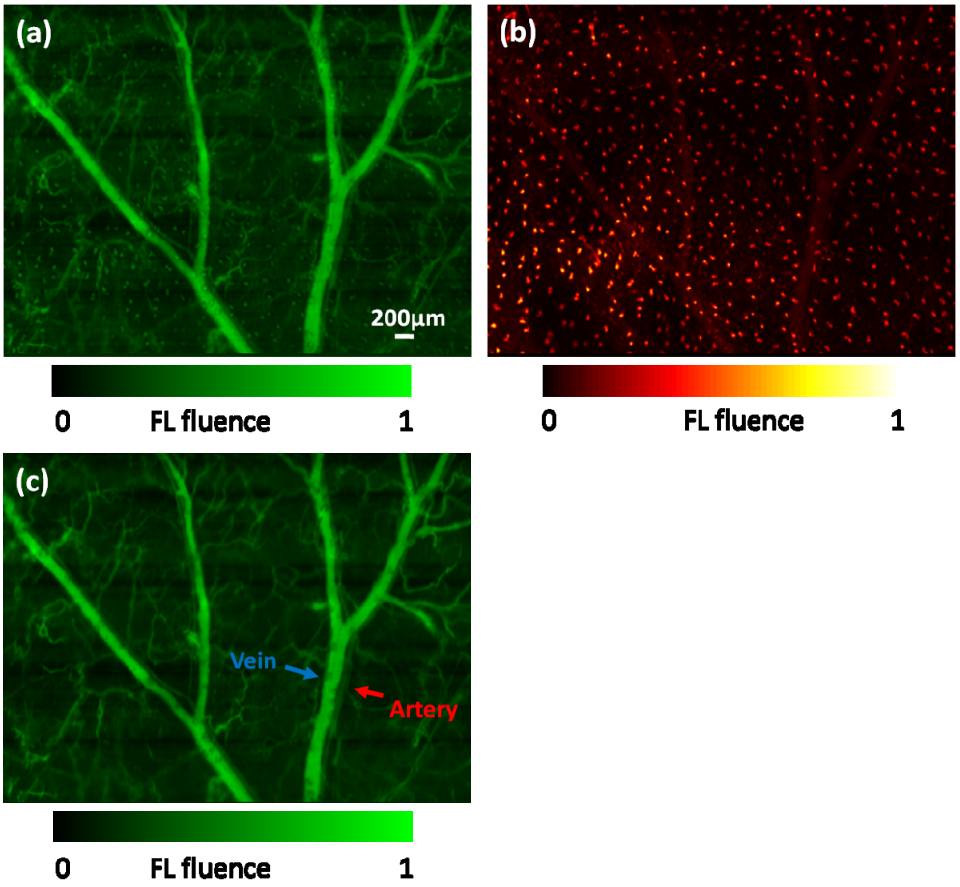

Figure 3. FCM imaging of a mouse ear *in vivo*. (a) FCM image of time-integrated phosphorescence excited at 523 nm. (b) FCM image of the sebaceous gland. (c) FCM image of the vasculature. FL: fluorescence.

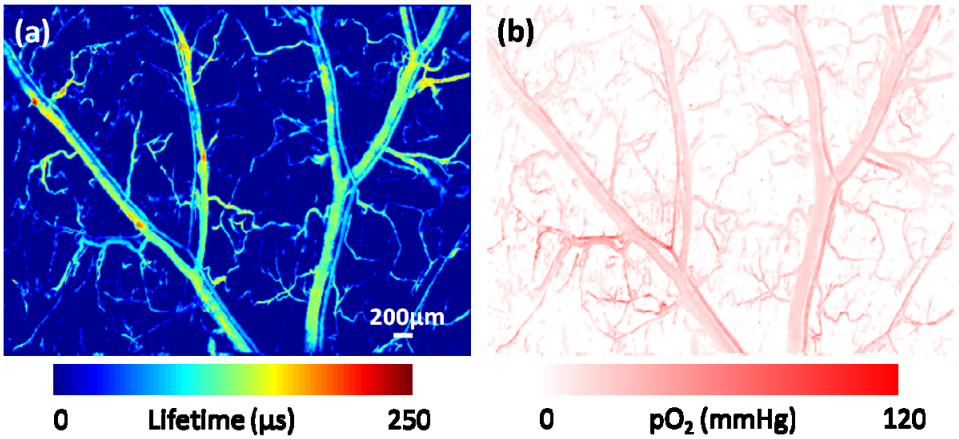

Figure 4. FCM imaging of a mouse ear *in vivo*. (a) FCM image of phosphorescence lifetime mapping. (b) FCM image of pO_2 mapping.

In summary, we demonstrate that the multi-modal PA-FCM imaging system provides complementary photoacoustic and fluorescence contrasts. Intrinsically co-registered PAM and FCM images can be acquired. Intravascular sO_2 and pO_2 levels, as well as total hemoglobin concentration, can be mapped vessel by vessel *in vivo*. Future study toward quantitative analysis of oxygen transport and consumption in tissues is very attractive.

ACKNOWLEDGEMENTS

We thank C. Zhang for helping with data processing and manuscript preparation, and Professor J. Ballard for careful proofreading. This work was sponsored in part by National Institutes of Health (NIH) grants R01 EB000712, R01 EB008085, R01 CA134539, U54 CA136398, and 5P60 DK02057933. L. Wang has a financial interest in Microphotoacoustics, Inc., and Endra, Inc., which, however, did not support this work.

REFERENCES

[1] Hu, S. and Wang, L. V., "Photoacoustic imaging and characterization of the microvasculature," J. Biomed. Opt. 15, 011101 (2010).
[2] Maslov, K., Zhang, H. F., Hu, S., and Wang, L. V., "Optical-resolution photoacoustic microscopy for in vivo imaging of single capillaries," Opt. Lett. 33, 929–931, (2008)
[3] Wang, L. V., "Multiscale photoacoustic microscopy and computed tomography," Nature Photon. 3, 503–509 (2009).
[4] Zhang, C., Maslov, K. and Wang, L., "Subwavelength-resolution label-free photoacoustic microscopy of optical absorption in vivo," Opt. Lett. 35, 3195–3197 (2010).
[5] Jiao, S., Xie, Z., Zhang, H. F., and Puliafito, C. A., "Simultaneous multimodal imaging with integrated photoacoustic microscopy and optical coherence tomography," Opt. Lett. 34, 2961–2963, (2009)
[6] Wang, Y., Maslov, K., Kim, C., Hu, S. and Wang, L. V., "Integrated photoacoustic and fluorescence confocal microscopy," IEEE Trans. Biomed. Eng. 57, 2576–2578, (2010).
[7] Lo, L-W, Koch, C. J. and Wilson, D. F., "Calibration of oxygen-dependent quenching of the phosphorescence of Pd-meso-tetra (4-carboxyphenyl) porphine: a phosphor with general application for measuring oxygen concentration in biological systems," Anal. Biochem. 236, 153–160 (1996).
[8] Yaseen, M., Srinivasan, V., Sakadzic, S., Wu, W., Ruvinskaya, S., Vinogradov, S. and Boas, D., "Optical monitoring of oxygen tension in cortical microvessels with confocal microscopy," Opt. Express 17, 22341–22350 (2009).

[9] Sakadžić, S., Roussakis, E., Yaseen, M., Mandeville, E., Srinivasan, V., Arai, K., Ruvinskaya, S., Devor, A., Lo, E., Vinogradov S. and Boas, D., "Two-photon high-resolution measurement of partial pressure of oxygen in cerebral vasculature and tissue", Nature Methods, 7, 755–759 (2010).
[10] Estrada, A., Ponticorvo, A., Ford, T. and Dunn, A., "Microvascular oxygen quantification using two-photon microscopy," Opt. Lett. 33, 1038–1040 (2008).
[11] Sinaasappel, M. and Ince, C., "Calibration of Pd-porphyrin phosphorescence for oxygen concentration measurements in vivo," J. Appl. Physiol. 81, 2297–2303 (1996).
[12] Adair, G., "The hemoglobin system: VI. the oxygen dissociation curve of hemoglobin," J. Biol. Chem. 63, 529–545 (1925).